International Journal of Mass Spectrometry 307 (2011) 3–15

Contents lists available at ScienceDirect

International Journal of Mass Spectrometry

journal homepage: www.elsevier.com/locate/ijms

Mass spectrometric imaging (MSI) of metals using advanced BrainMet techniques for biomedical research☆

Johanna Sabine Becker[a,*], Andreas Matusch[b], Julia Susanne Becker[c], Bei Wu[a,1], Christoph Palm[d], Albert Johann Becker[e], Dagmar Salber[b]

[a] Central Division of Analytical Chemistry, Forschungszentrum Jülich, D-52425 Jülich, Germany
[b] Institute of Neurosciences and Medicine (INM-2 and INM-4), Forschungszentrum Jülich, D-52425 Jülich, Germany
[c] Aeropharm GmbH, D-07407 Rudolstadt, Germany
[d] Faculty of Computer Science and Mathematics, Regensburg University of Applied Sciences, D-93053 Regensburg, Germany
[e] Department of Neuropathology, University of Bonn Medical Center, Germany

ARTICLE INFO

Article history:
Received 29 November 2010
Received in revised form 18 January 2011
Accepted 18 January 2011
Available online 26 January 2011

Keywords:
Bioimaging
Brain tissue
Laser ablation inductively coupled plasma mass spectrometry
Laser microdissection inductively coupled plasma mass spectrometry
Metals
Metallomics
Nano-LA-ICP-MS
Tumour

ABSTRACT

Mass spectrometric imaging (MSI) is a young innovative analytical technique and combines different fields of advanced mass spectrometry and biomedical research with the aim to provide maps of elements and molecules, complexes or fragments. Especially essential metals such as zinc, copper, iron and manganese play a functional role in signaling, metabolism and homeostasis of the cell. Due to the high degree of spatial organization of metals in biological systems their distribution analysis is of key interest in life sciences. We have developed analytical techniques termed BrainMet using laser ablation inductively coupled plasma mass spectrometry (LA-ICP-MS) imaging to measure the distribution of trace metals in biological tissues for biomedical research and feasibility studies—including bioaccumulation and bioavailability studies, ecological risk assessment and toxicity studies in humans and other organisms. The analytical BrainMet techniques provide quantitative images of metal distributions in brain tissue slices which can be combined with other imaging modalities such as photomicrography of native or processed tissue (histochemistry, immunostaining) and autoradiography or with in vivo techniques such as positron emission tomography or magnetic resonance tomography.

Prospective and instrumental developments will be discussed concerning the development of the metalloprotein microscopy using a laser microdissection (LMD) apparatus for specific sample introduction into an inductively coupled plasma mass spectrometer (LMD-ICP-MS) or an application of the near field effect in LA-ICP-MS (NF-LA-ICP-MS). These nano-scale mass spectrometric techniques provide improved spatial resolution down to the single cell level.

1. Introduction

Mass spectrometric imaging (MSI) is a new emerging field that provides unmatched capabilities for distribution studies of trace metals and bio-molecules. Their identification and characterization in biomedical tissue and in cells is of key interest in life science studies [1–4]. It is known that trace metals (e.g., zinc, copper and iron) are involved in cellular processes like proliferation, myelinization and signaling essential for the growth and functioning of the brain. Approximately one-third of all proteins are believed to require metals, often as essential components of the catalytical centre of enzymes [5]. On the other hand disturbed metabolism of these metals is a key feature in several diseases. Metals catalyse central pathomechanisms in neurodegenerative diseases such as the oligomerization and formation of proto-fibrils of amyloid Aβ in Alzheimer's disease and of α-synuclein in Parkinson's disease. In the insoluble higher aggregates thereof impressing as plaques, fibrils and Levy bodies high accumulations of metals were detected using microlocal analytical techniques. Furthermore, metal content and distribution appear highly dynamical during processes such as ischemia or normal ageing [6–10].

Examples, where metals are not disease modifiers but the protagonists are Menkes and Wilson disease caused by a disruption in copper efflux pumps. Whereas in X-linked Menkes disease a defect of ATP7A, of ubiquitous expression, results in the failure of enteral resorption and consecutive global Cu deficiency, in Wilson disease of autosomal recessive inheritance a defect of ATP7B results – due

☆ BrainMet—Bioimaging of Metals in Brain and Metallomics.
* Corresponding author. Tel.: +49 2461 612698; fax: +49 2461 612560.
E-mail address: s.becker@fz-juelich.de (J.S. Becker).
[1] Alexander von Humboldt postdoctoral research fellow.

1387-3806/$ – see front matter © 2011 Elsevier B.V. All rights reserved.
doi:10.1016/j.ijms.2011.01.015

to failing cellular excretion – in an accumulation of Cu in the liver, the brain and other tissues.

Metal-containing drugs have been used and are developed for the treatment of diseases such as cytostatic platinum derivatives against tumours, lithium as mood stabilizer, gold complexes against rheuma and vanadate against diabetes [11,12]. A series of metals – especially lanthanide – complexes are developed as contrast agents or photosensitizers. Finally, trace metals of high cyto- and neurotoxicity like cadmium, arsenic, mercury and lead play a role in toxicology and occupational medicine [13,14]. In all these cases of non-physiological exogenous metal applications knowledge of the local and microlocal distribution is the key of a targeted deployment.

Investigation of trace metal distributions in brain tissue requires powerful quantitative imaging techniques. There are a few widely accepted analytical techniques – like X-ray spectroscopic techniques for biological tissues [15,16], scanning electron microscopy with energy-dispersive X-ray analysis (SEM-EDX), X-ray fluorescence analysis using synchrotron radiation facilities (SRXRF) [17–20] or proton-induced X-ray emission (PIXE) [13] and secondary ion mass spectrometry (SIMS) [21–25] – to measure the distribution of trace metals in biological tissues. Among the MSI techniques for biomolecules, matrix-assisted laser desorption/ionization mass spectrometry (MALDI-MS) [26–30] is well established. This technique allows imaging of small molecules and large biomolecules up to an m/z range of over 100 000 Da within biological systems. The application of MALDI-IMS as an imaging technique has grown rapidly, enhanced by the recent introduction of commercial instrumentation and devices for sample preparation and data acquisition and analysis [31]. Tissue imaging at atmospheric pressure by desorption electrospray ionization imaging mass spectrometry (DESI-MS) was created by Cooks' working group [32,33].

Laser ablation inductively plasma mass spectrometry (LA-ICP-MS) was created for quantitative imaging of trace elements in biological materials (with a spatial resolution down to 10 μm) providing accurate and reliable data for quite different applications [7,10]. A brief overview and comparison of these instrumental analytical imaging techniques applied to biological tissues and cells in the low-micrometer and nanometer range is given in a review by Wu and Becker [34] within this special issue.

The rapidly growing interest in studying neurodegenerative diseases and metal distribution has been increasing rapidly with the development of imaging techniques during the last 5 years [3] and is becoming the object of fundamental developments and research in various institutions throughout the world [22,35–37]. The established BrainMet techniques using LA-ICP-MS at Forschungszentrum Jülich have been employed for many applications in brain research. [8,9,38,39] In previous studies, we demonstrated the BrainMet techniques providing valid and plausible distribution images of numerous metals, metalloids (Se, As, Sb and Te) [40] and selected non-metals (C, P, S, Cl and I) in tissue sections. Quantitative metal distributions were mapped in healthy and diseased human and rodent brain affected by Alzheimer's disease, Parkinson's disease, stroke, depression, epilepsy, tumours – such as glioblastoma multiforme in humans and rats [9,41–45] – and across normal ageing in rats [6,8,46]. Furthermore, the BrainMet techniques have been employed in single hair analysis to monitor contaminations of toxic metals and therapeutic drugs [47] and in numerous metallomics studies [48,49].

The aim of this review is to illustrate the different facets and especially novel applications of the BrainMet techniques created at Forschungszentrum Jülich by investigating the metalloarchitecture of native brain cryo-sections. The benefits of analytical BrainMet techniques will be demonstrated on selected biomedical tissue samples spanning a wide range of spatial dimensions.

2. Experimental setup

For mass spectrometric bioimaging studies by LA-ICP-MS a commercial laser ablation system using a solid-state Nd:YAG laser (from New Wave, Fremont, CA, working at wavelengths of 266 nm) was coupled directly via a connection tube to the ICP torch of a quadrupole-based inductively coupled plasma mass spectrometer (ICP-QMS) with collision cell (Agilent 7500ce, Agilent or XSeries 2, Thermo Fisher Scientific, Bremen). During ablation native biological tissue was kept at room temperature. For imaging of dried native tissue no cooled (cryo) laser ablation chamber was required such as developed for the analysis of fresh wet biological specimens in author's lab [50]. The instrumental setup of high-tech BrainMet techniques using a conventional new laser ablation system from New Wave (NWR 213) coupled to a quadrupole-based ICP-MS (XSeries 2, Thermo Fisher Scientific) for application in routine measurements and the arrangement of the novel emerging metalloprotein microscopy for detection of metals in small size tissue and single cells are summarized in Fig. 1.

The workflow of bioimaging of tissue by LA-ICP-MS techniques including sample preparation by cryo-cutting, mass spectrometric measurements (line by line scanning), generation of images and the quantification procedure was illustrated in the previous review [10]. The new laser ablation system NWR 213 compared to the New Wave UP 266 applied in former experiments offers an enlarged laser ablation chamber (10 cm × 10 cm—for study of large sample size), higher scan speed and more effective ablation and transport of ablated material to the ICP source. These advantages resulted in a significant enhancement of sensitivity at smaller spot size. Mass spectrometric measurements by LA-ICP-MS for two-dimensional (2D) imaging of biological tissues were performed by line scanning ablation (line by line) of thin tissue sections with a focused laser beam as described before [7].

In the first experiment using the new LA-ICP-MS setup (shown in Fig. 1) quantitative bioimaging of metals in native mouse spinal cord cryosections with sample dimensions of 2.3 mm × 1.5 mm resulted in the "butterfly" shape of the central grey matter with higher concentrations of the transition metals Fe, Mn, Cu and Zn compared to white matter [51].

In order to improve the spatial resolution of imaging analysis of metals within tissue the development of metalloprotein microscopy is proposed. The laser microdissection apparatus SmartCut Plus LMD (MMI Molecular Machines and Industries, Zurich, Switzerland) with an inserted small laser ablation chamber coupled to ICP-MS was described in a previous experiment [52]. The LMD is a microscope-based analytical tool using a high-precision laser beam to selectively isolate specific cell types, individual cells or cell organelles from tissue sections on a glass substrate. The microscope of LMD is employed to visualize small structures or single cells of interest.

3. Image generation

The interactive software solution for Image Generation and Analysis (IMAGENA) was developed to convert the continuous stream of LA-ICP-MS raw data into two-dimensional images present in a common file format. The software is able to adjust the spatial domain in terms of image width and height as well as pixel size properly knowing system parameters like number of measurements, acquisition time of a single mass spectrum and the probe table propagation speed. Especially the possibility of floating point values for the line length proved valuable to overcome the asyn-

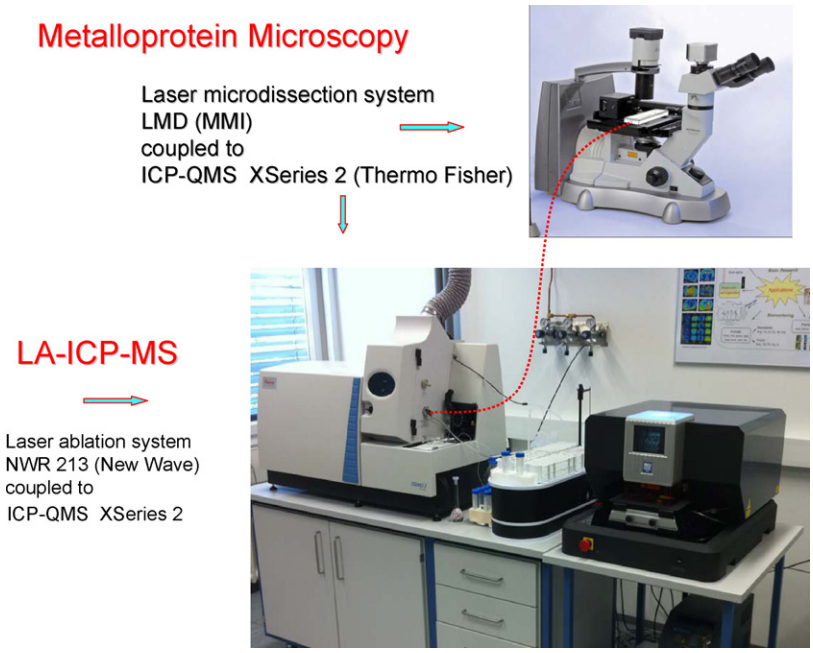

Fig. 1. Experimental setup of the techniques created at BrainMet using a conventional ICP-MS. Either the laser ablation system NWR 213 (New Wave Research, Fremont) was coupled to a quadrupole-based ICP-MS XSeries 2 (Thermo Fisher Scientific, Bremen) or within the setup of a metalloprotein microscope a laser microdissection apparatus (SmallCut, MMI, Zuerich) with a small dedicated ablation chamber inserted.

chrony of table propagation and acquisition cycle frequency of the mass spectrometer.

A linear calibration procedure to calculate the total element concentration in the sample is integrated. Additionally, *y*-drifts that occur occasionally in single datasets are corrected by a piecewise linear function with manually adjustable anchor points. IMAGENA provides a visual feedback for all processing steps by the visualisation unit. The adjustment of minimum, maximum as well as mean value allows contrast enhancement, noise reduction and the handling of artificial single value outliers. IMAGENA proved its suitability and usefulness in more than 2 years of routine use.

Fig. 2 shows the graphical user interface of Imaging Generation software (IMAGENA) developed at Forschungszentrum Jülich. More details of software development for LA-ICP-MS imaging generation are described in another paper of this issue [53].

4. Quantification procedures

LA-ICP-MS allows easy quantification procedures if suitable standard references materials (SRM) are available. However, for the imaging analysis of biomedical tissue sections no SRMs are available. Therefore, quantification of analytical data is performed using a set of matrix-matched homogenized laboratory standards with well-defined added metal concentrations of 41 analytes within a biologically relevant range (e.g., 0, 6, 12, 18, 24 and 30 $\mu g\,g^{-1}$ added Zn) as exemplified in Fig. 3. For this purpose 15 mouse brains were homogenized, portioned, spiked with dilutions of a multielement solution, homogenized again, frozen, cryo-sectioned at a thickness of 30 μm and placed onto glass slides that later can accommodate the sample sections of interest. The set of lab standards (shown on the right top of glass slide in Fig. 2) and the mouse brain tissue (left) of 30 μm thickness were analyzed together under the same experimental conditions by LA-ICP-MS imaging in routine mode in the BrainMet laboratory as described elsewhere [9]. Five parallel LA-ICP-MS line scans through the standard bars were acquired as illustrated in the time-resolved mass spectra of $^{64}Zn^+$ and $^{63}Cu^+$, left bottom of Fig. 3. The regression coefficients of the calibration curves resulting from averaging the five line scans were better than 0.99 for essential transition metals as exemplified for $^{64}Zn^+$ in Fig. 3, right bottom. From the calibration curve the concentration of analyte in the original un-spiked brain mixture (tissue blank) is given by the intersection with the *x*-axis. This value and the final metal concentrations in the prepared laboratory standards were verified by ICP-MS after microwave-induced digestion and their homogeneity was investigated using LA-ICP-MS imaging.

Another possibility for element quantification in brain tissue and single hair analysis is the SRM-free approach of solution-based calibration in LA-ICP-MS that was developed recently in the BrainMet laboratory [54,55]. The experimental arrangement is shown in Fig. 4. A dual argon flow of the carrier gas and nebulizer gas is applied. A dry aerosol produced by laser ablation of biological sample and an aqueous aerosol generated by pneumatic nebulisation of standard solutions are carried by two different flows of argon as carrier or nebulizer gas, respectively, and introduced separately in the injector tube of a special ICP torch, through two separated apertures. Both argon flows are mixed directly in the ICP torch. External calibration via defined standard solutions before distribution analysis of brain tissue or single hair was employed as calibration strategy. A correction factor, calculated using hair with known analyte concentration (measured by ICP-MS), was applied to correct the different elemental sensitivities of ICP-MS and LA-ICP-MS.

5. Figures of merit of the developed BrainMet techniques

The figures of merit with respect to the application fields, sample type, size and preparation, mass range and resolution, depth of an ablated line, spatial resolution and limits of detections (LODs), fractionation and matrix effects, quantification possibilities, precision of metal distribution, measurement time, and software of the LA-ICP-MS imaging technique are summarized in Table 1. LA-ICP-MS imaging techniques have advantages over MALDI-MS imaging: native biological tissue can be measured directly, and no sample preparation is required, which means no matrix application is required as in MALDI-MS. A comparison of the figures of merit of instrumental analytical imaging techniques applied to biological tissues and cells in the low-micrometer and nanometer range

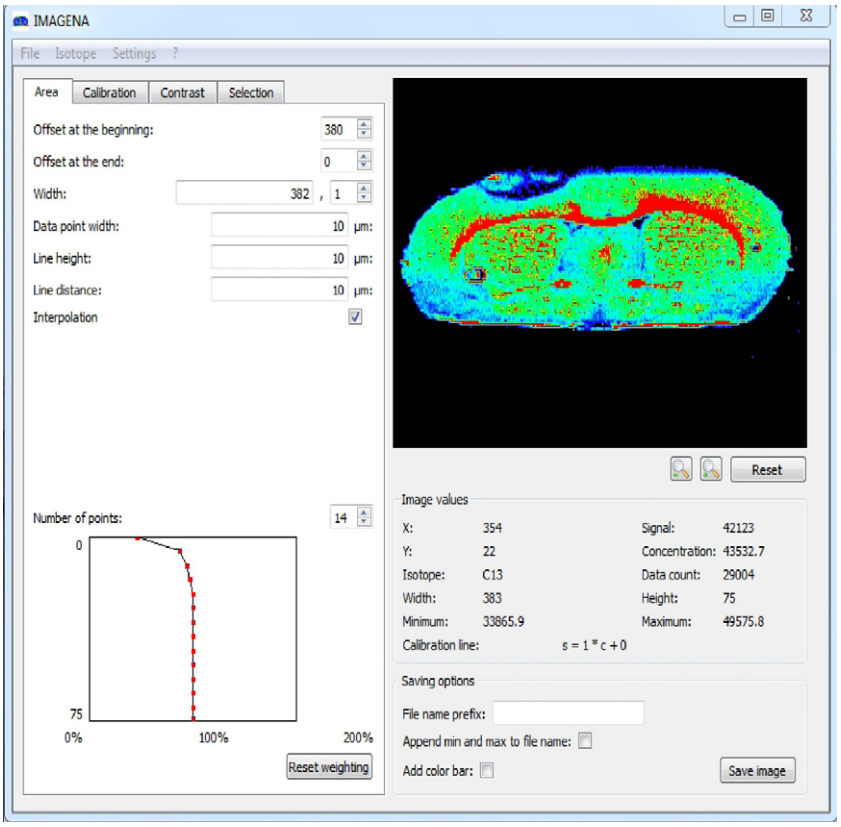

Fig. 2. Graphical user interface of Image Generation software (IMAGENA). The main menu is shown allowing to set spatial parameters of image reconstruction, to apply a weighting function for *y*-drift correction and data saving options. The reconstructed image together with actual quantitative parameters is displayed.

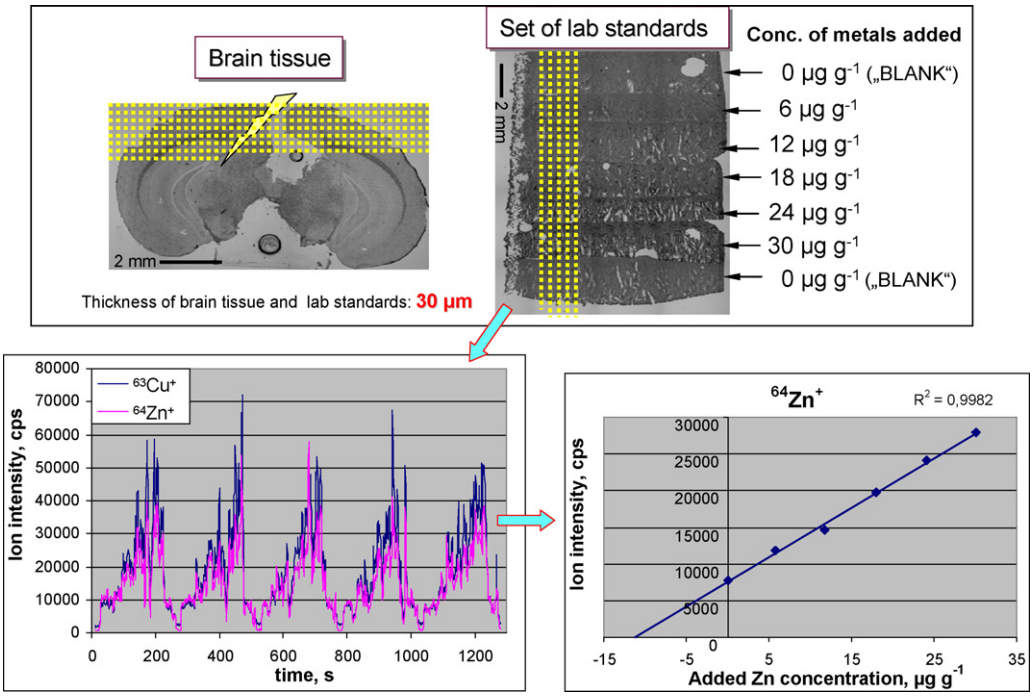

Fig. 3. Calibration procedure using matrix-matched laboratory standards. Together with the sample that is ablated line-by-line (top left) a set of standard slices is placed into the ablation chamber and measured before and after the sample by ablating five parallel lines. The standards are cryo-sections from a bloc casted of brain tissue homogenates spiked with 41 analytes of interest at concentrations within a range relevant to biological samples as exemplary indicated for Zn (top right). The ion intensities measured during the five subsequent line scans are plotted at the bottom left. At the bottom right a calibration curve obtained for Zn measuring the set of laboratory standards is shown. As can be seen fissures in the homogenate sections are drying artefacts and virtually averaged out over the ~2 mm width of each bar of standard material.

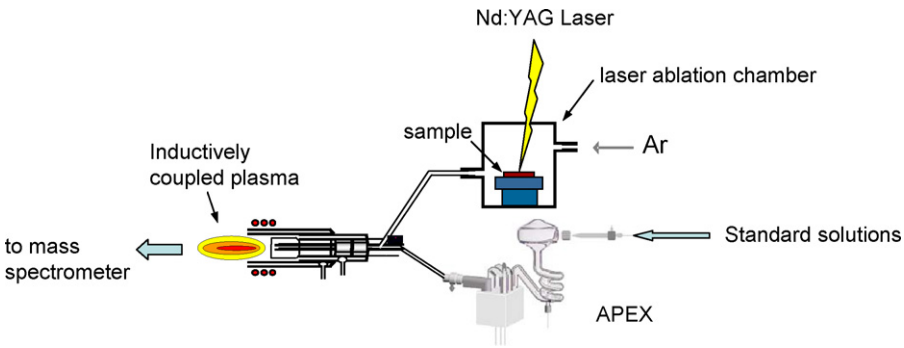

Fig. 4. Experimental setup of solution based calibration. The two flows of ablated sample and nebulized standard solution were unified at the entrance of the central tube of the plasma torch.

Table 1
Figures or merit of LA-ICP-MS imaging of tissue figures or merit of LA-ICP-MS imaging of tissue.

Sample type	Native cryo-sections on glass slides
Sampling	Laser ablation of tissue (line by line) at atmospheric pressure in LA chamber
Sample size (max.)	100 mm × 100 mm (complete ablation of tissue)
Sample preparation	None
Mass range	6–250 Da
Mass resolution ($m/\Delta m$)	ICP-QMS: 300; ICP-SFMS[a]: 300, 3000, 12000
Depth of ablated lines	=section thickness: <100 μm
Spatial resolution	5–120 μm
Limits of detection (LODs)	0.001–1 μg g^{-1}
Fractionation effects	None
Matrix effects	Less than one order of magnitude
Quantification of images	Easy; needs homogeneous reference materials
Precision of metal distribution	5–10%
Isobaric interferences	Low and rare due to dry sample material; subtracted as constant background or resolved by ICP-SFMS
Measurement time	4 h/cm^2
Software	IMAGENA [53]
Image generation	Of preselected masses defined before imaging
Application fields	Multielement determination of trace, minor and major elements in biological tissue, isotope ratios

[a] ICP-SFMS—double focusing sector field ICP-MS.

is discussed in the following paper [34]. Due to the multielement capability of LA-ICP-MS, nearly all trace and minor elements can be analyzed directly in one measurement of the tissue section. The developed BrainMet techniques are robust and provide reliable and reproducible data for metal distributions in native biological tissue slices and have been applied for studying the distribution of essential metals (Cu, Zn, Fe, Mn, Na, Ca, K, Mg, etc.), toxic metals (Cd, Hg, Pb, U and Th), non-metals (C, S, P, Cl and I) and metalloids (As and Se). We investigated native tissue sections of a thickness between 10 and 40 μm. Detection limits for metals in LA-ICP-MS images after ablation at a laser spot size of 100 μm in the range of 0.01–0.3 μg g^{-1} were obtained. In general, the structural information mutually provided by a set of multielement LA-ICP-MS images of rat or mouse brain slices exceeded that provided by conventional histological staining techniques and was categorized using anatomical brain atlases (e.g., Paxinos and Watson's mouse or rat brain atlas) [56] used in brain research laboratories.

Examples of metal imaging of samples with decreasing size spanning from a huge human brain hemisphere measured in a large laser ablation chamber, via rat and mouse brain and mouse spinal cord sections using conventional LA-ICP-MS techniques to a selected subregion within a rat brain affected by photo-induced stroke and down to single nerve cells by metalloprotein microscopy – this is the future goal in the development of BrainMet techniques – are illustrated in Fig. 5.

6. Application fields of BrainMet techniques

The different application fields of LA-ICP-MS imaging techniques developed at Forschungszentrum Jülich in brain research were described in a series of previous publications [1,6,8,9,57] and are summarized in Fig. 6. In this figure, the following applications of imaging LA-ICP-MS are shown (from top left in clockwise direction): the Cu and Fe image of a mouse model for Alzheimer's and Parkinson's disease, respectively, the Zn distribution in a rat brain bearing a tumour after gamma knife irradiation and after photo-induced stroke, the Na image in coronal rat brain section with hematoma, the Cu distribution in a horizontal section of a normal rat brain, the Li distribution in a mouse brain after i.p. application of Li, the Cu image in an old mouse brain in the frame of ageing studies, the Cu image in the hippocampus from patient who underwent surgery for epilepsy and the Fe distribution in a rat model of Chorea Huntington.

6.1. Distribution of metals in human hippocampus

The iron, copper and zinc distribution in a resection from a human hippocampus is illustrated in Fig. 7. The tissue was obtained from a patient who suffered from pharmaco-resistant temporal lobe epilepsy (TLE) and underwent epilepsy surgery for seizure control [58]. The hippocampal formation showed the lesion pattern of hippocampal sclerosis (HS), i.e., neuronal degeneration and reactive astrogliosis [59]. The results of averaging the concentrations across free-hand drawn regions of interest along anatomical boundaries using PMod Software v3.0 as illustrated in Fig. 7 are summarized in Table 2. Large parts of the typical metalloarchitecture were preserved. Break lines in the layering pattern allowed a precise delineation of the different segments of the cornu ammonis (CA1–4). In contrast to results of Timm's autometallography for Zn that labels free Zn and a more or less arbitrary fraction of bound Zn it can be stated that the high total Zn concentration does not occur in the stratum lucidum of CA3, but in the stratum pyramidale of CA3 and in the inner layers of the fascia dentata. The precise co-localization of metals with the damage pattern of HS, which imposes as a loss in pyramidal cell bodies particularly in CA1 and CA3/4 with concomitant reactive astrogliosis is subject of ongoing examinations.

6.2. Mapping the physiological metallo-architecture of the brain

The brain is especially rich in substructures that display a very distinct inventory in metals. Elemental imaging resolves a large

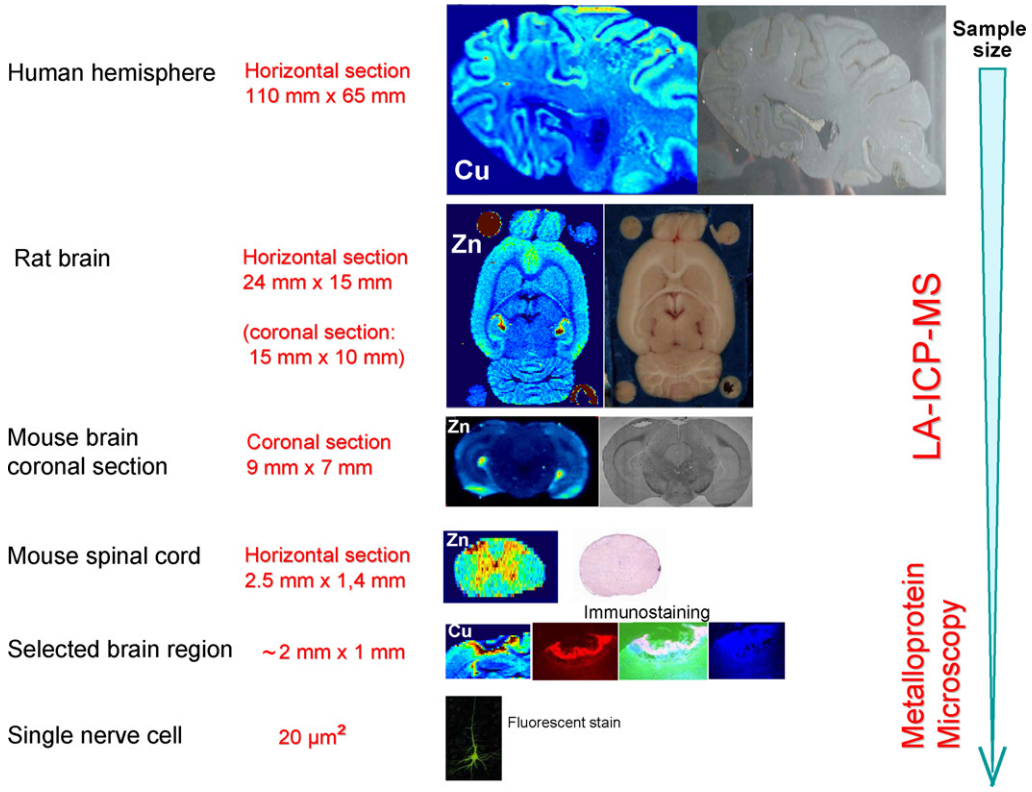

Fig. 5. Examples of metal imaging of biomedical tissue of decreasing size spanning from a huge human brain hemisphere placed in a large laser ablation chamber, via rat and mouse brain sections and mouse spinal cord using a conventional LA-ICP-MS technique to metalloprotein microscopy while analyzing selected regions of photo-induced stroke in rat brain. Our main future goal is given by the analysis of single nerve cells.

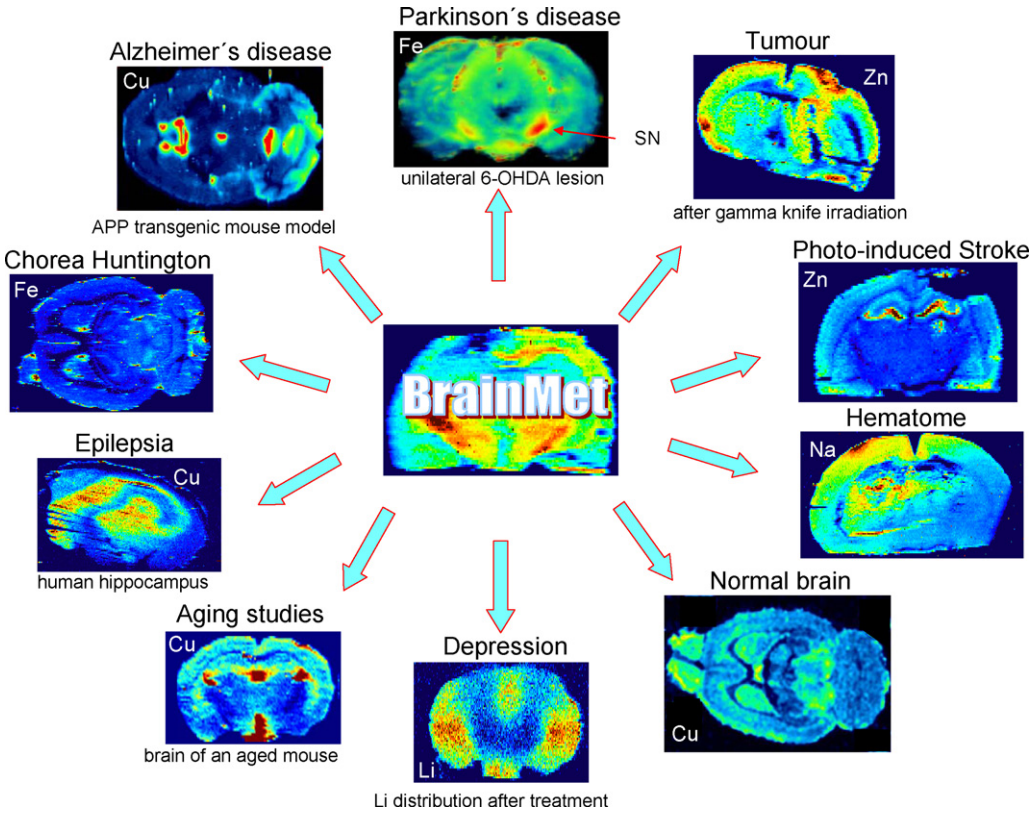

Fig. 6. Different application fields of BrainMet techniques (from top left in clockwise direction): Cu image of Alzheimer's and Fe image of Parkinson's mouse brain, Zn distribution in rat brain with tumour after gamma knife irradiation and photo-induced stroke, Na image in a coronal rat brain section with hematoma and Cu distribution in a horizontal section of normal rat brain, Li in a mouse brain after treatment, Cu in an old mouse brain in the context of ageing studies, Cu in the hippocampus of a human patient who underwent surgery for temporal lobe epilepsy and Fe distribution in a rat model of Chorea Huntington, horizontal brain section.

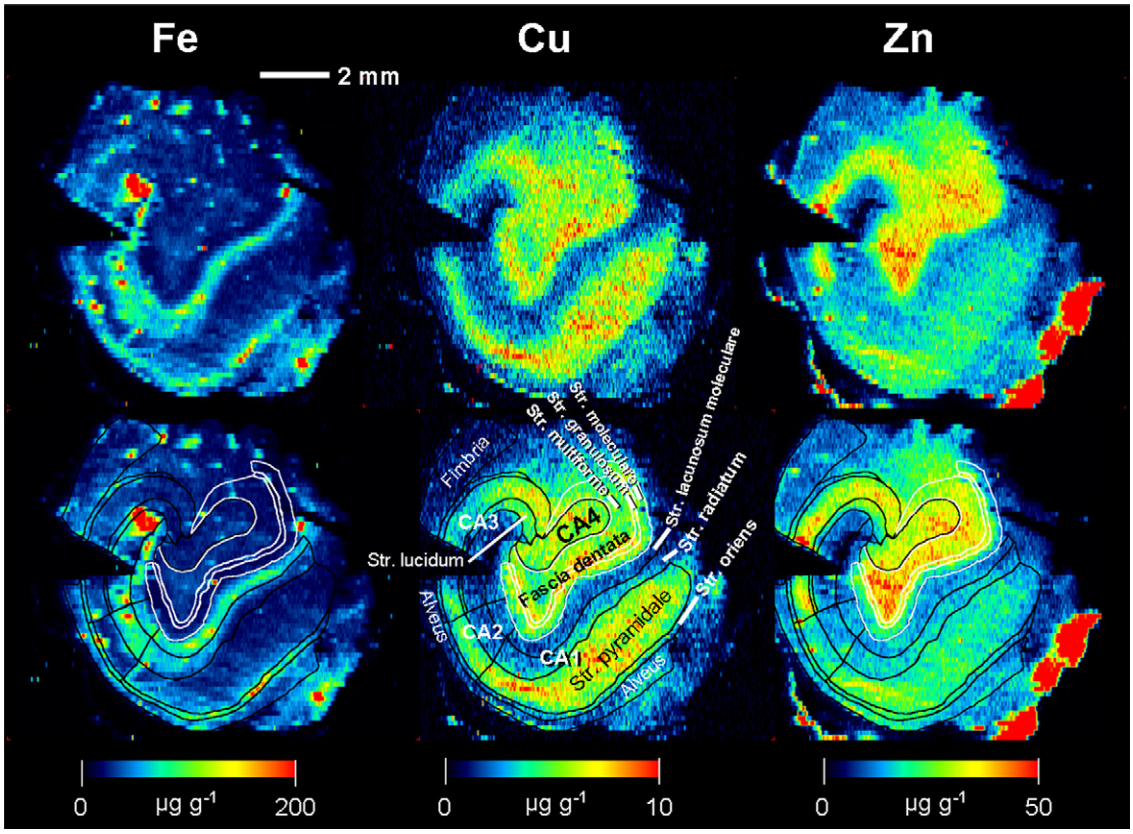

Fig. 7. Images of iron, copper and zinc in human hippocampus measured by LA-ICP-MS imaging. In the lower row anatomically defined regions of interest are delineated, the average concentrations of which are given in Table 2. Note the sharp discrimination of layers and the break lines in the layering pattern defining the extension of different segments of the cornu ammonis (CA).

number of cerebral nuclei and layers often of sharp limitation which are hard to discriminate in standard stained sections. This is exemplified in Fig. 8 at a horizontal rat brain section. As a surplus, this sample, very rich in details, gives an impression of the spatial resolution capabilities of LA-ICP-MS. The filigree branches of the cerebellar lobules termed arbor vitae were resolved in the maps of all elements assessed. Multiple thalomo-mesencephal subnuclei show an enrichment of Mn and are resolved in the Mn image. The Zn-image very sharply shows the polymorph layer of the fascia dentata in continuity with the lucidum layer of CA3. Fe is displayed at a large concentration range window contrasting the blood vessels of the circulus Wilisi from the brain parenchyma. The Fe concentration in blood amounts to 400 $\mu g\,g^{-1}$ wet weight whereas in brain tissue typically 5–20 $\mu g\,g^{-1}$ occur.

Table 2
Metal concentrations determined by quantitative LA-ICP-MS imaging in selected layers of a resection from a sclerotic human hippocampus of a patient suffered from epilepsy.

	CA1	CA2	CA3	CA4	FD
Fe, $\mu g\,g^{-1}$					
Str. oriens	76	74	48		mult.: 30
Str. pyramid.	33	46	36		gran.: 26
S. radiatum	42	80	97		
S. lac.-mol	81				mol.: 36
Alveus	44			30	
Zn, $\mu g\,g^{-1}$					
Str. oriens	18	20	48		mult.: 37
Str. pyramid.	20	18	36		gran.: 30
S. radiatum	16	15	97		
S. lac.-mol	13				mol.: 15
Alveus	14			33	
Cu, $\mu g\,g^{-1}$					
Str. oriens	3.5	2.8	2.4		mult.: 5.2
Str. pyramid.	6.0	4.4	4.3		gran.: 6.4
S. radiatum	3.1	2.3	2.0		
S. lac.-mol	2.0				mol.: 3.4
Alveus	1.8			6.1	

Str., stratum; pyramid., pyramidale; lac.-mol., lacunosum-moleculare; CA, cornu ammonis; FD, fascia dentata; mult., stratum multiforme; gran., stratum granulosum; mol., stratum moleculare.

6.3. Elemental distribution in a rat model of Parkinson's disease

LA-ICP-MS has been employed previously in the mouse MPTP toxic model of Parkinson's disease [9]. Ongoing studies assess the 6-OHDA mouse and rat model of Parkinson's disease. As a preview of this forthcoming work a reconstruction of a 3D stack of Fe-maps of an unilaterally lesioned animal is displayed in maximum intensity projection within Fig. 6 (top). A study in this special issue [60] suggests that formalin fixed human tissue is still accessible to LA-ICP-MS imaging yielding plausible concentrations of Fe and Mn. This would allow to exploit neuropathological collections of well characterized human case series. Major questions in this context are the relevance of metals in the pathogenesis, whether animal models appropriately reflect this feature of human pathophysiology and the possible therapeutic impact of metal chelators and anti-oxidants.

6.4. Bioimaging of rat brain with stroke

Metal imaging in the Watson photothrombosis model of stroke was the subject of a previous paper [1]. After systemic application of a photosensitizer, cortical arteries were occluded using local white light illumination. High increases of Cu, Fe, Zn, Ni

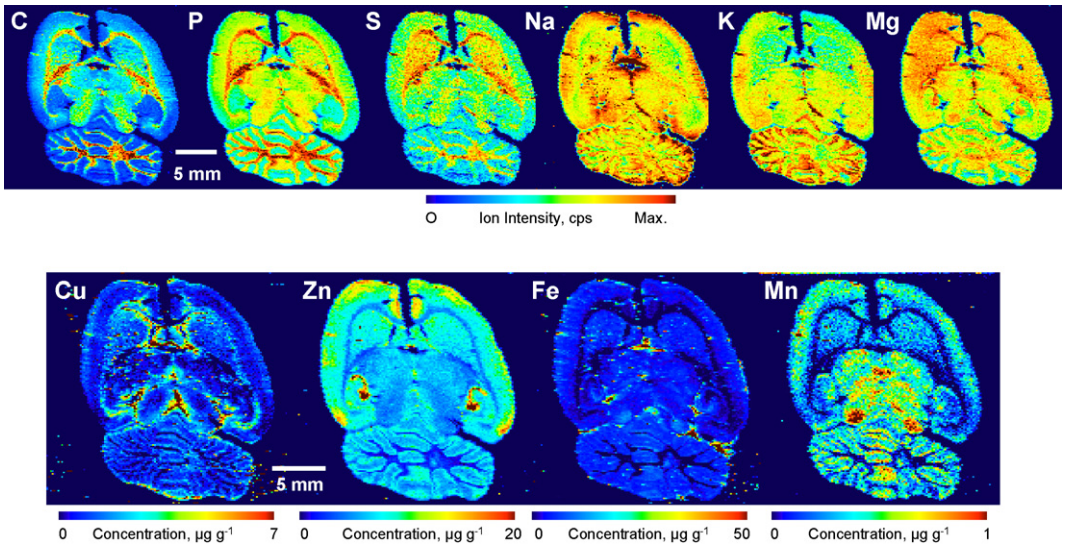

Fig. 8. Horizontal section of a rat brain crossing the colliculus superior, thalamus and striatum. The filigree branches of the cerebellar lobules termed arbor vitae were resolved in the maps of all elements assessed. Multiple thalomo-mesencephal subnuclei show an enrichment of Mn and are resolved in the Mn image. The Zn-image very sharply shows the polymorph layer of the fascia dentata in continuity with the lucidum layer of CA3. Fe is displayed at a large concentration range window contrasting the blood vessels of the circulus Wilisi from the brain parenchyma.

and Ti were observed in the demarcation zone surrounding the necrotic infarct area. Surprisingly a thalamic enrichment of Mn and Ti pointed to phenomena of retro- and anterograde degeneration as a response to cortico-thalamic disconnection. Fig. 9 exemplifies these findings in a coronal section that crosses the demarcation zone and the thalamus. Further investigations on the kinetics of this lesion and multimodal imaging are in progress.

6.5. Study of a rat brain with a mono-hemispherical tumour

Cultured tumour cells of the fast growing glioblastoma line F98 were stereotactically injected into the striatum [42–45]. After 3 weeks of tumour proliferation the animals received a local irradiation of 20 Gy by a gamma knife which consisted of many radiation sources directed onto one sharp focus of mm dimension. Fig. 10 summarizes the distribution of the transition metals (Cu, Zn, Fe

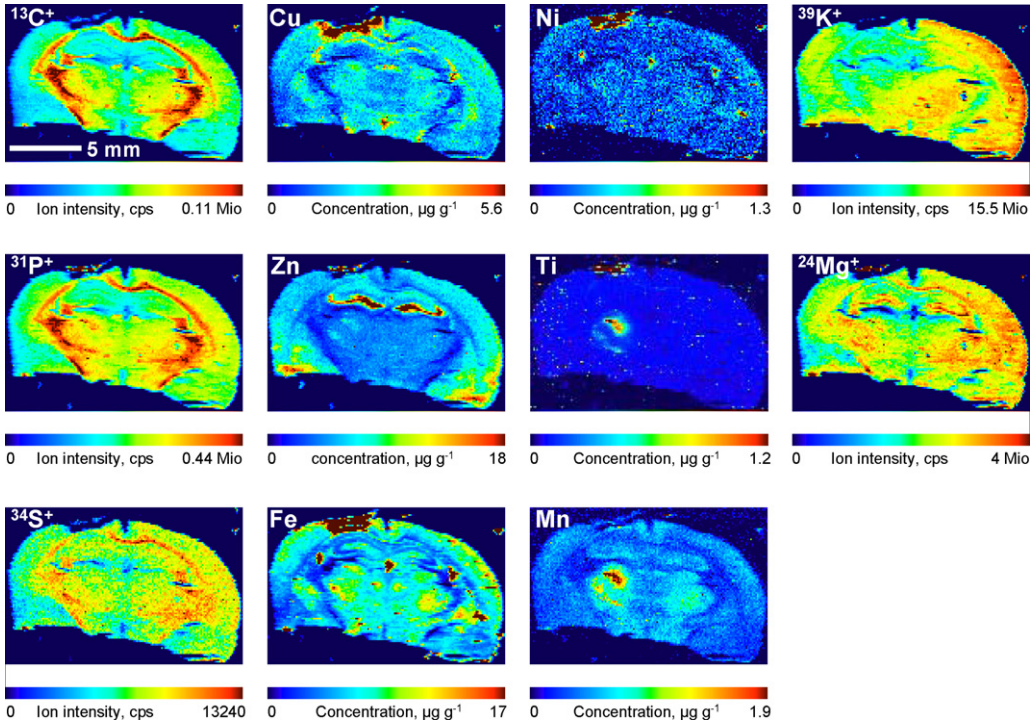

Fig. 9. Coronal section across the demarcation zone of a photoinduced thrombosis according to the Watson model of stroke. Note the enrichment of a series of metals in the infarct demarcation zone at the upper left edge of the brain and the enrichment of Mn and Ti in the thalamus – in the centre of the brain distant from the lesion – a degenerative consequence of thalamo-cortical disconnection.

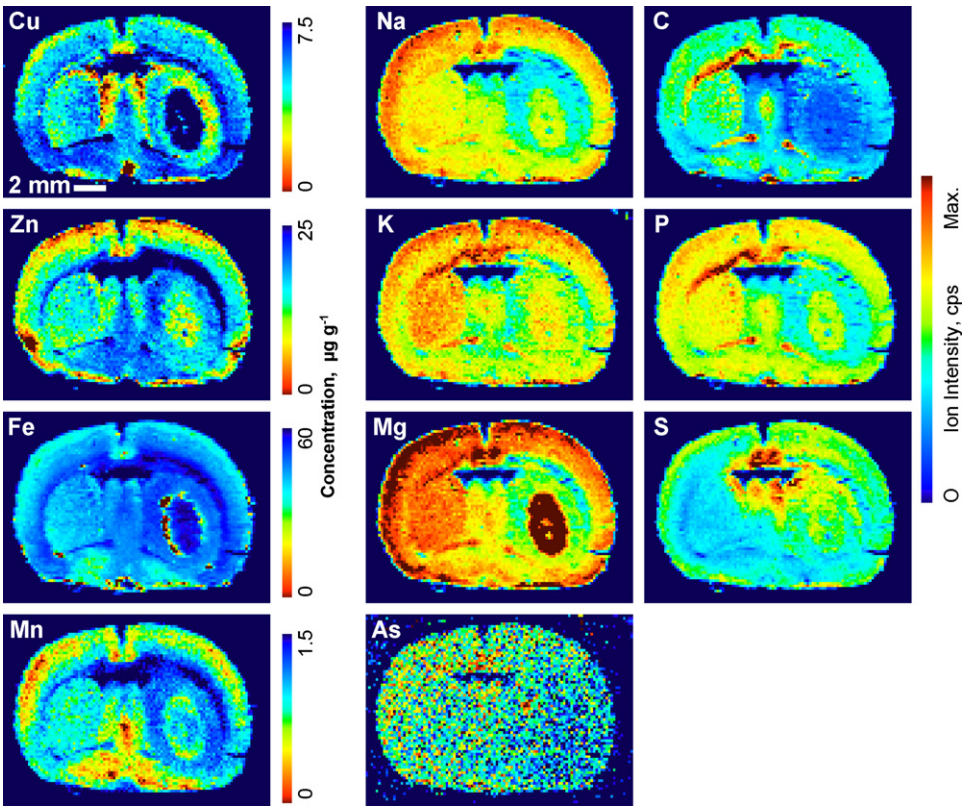

Fig. 10. Images of selected metals (Cu, Zn, Fe, Mn, Na, K, Mg and As) and non-metals (C, P and S) in a rat brain section bearing a gamma irradiated F98-tumour. From the centre to the periphery of the tumour can be discriminated a necrosis, a solid and a demarcation zone. The tissue surrounding the tumour shows substantial edema as suggested by the lower carbon and thus higher water content. Note the clear compression of the contralateral hemisphere.

and Mn) the alkali metals (Na and K) the earth alkali metal Mg and non-metals (C, P and S) in a rat brain with a tumour region. In addition, the tumour was detected by autoradiography with the PET-tracer [^{18}F]fluoroethyl tyrosine ([^{18}F]FET) as described in a previous paper [1]. LA-ICP-MS imaging allowed to discriminate four zones: a central necrotic zone without sharp delimitation containing high Zn and comparatively low Mn, Cu, Fe, K, P and S, an inner solid zone with medium Zn, high Mg, Mn, Na, K, P, S and low Cu and Fe, a capsular demarcation zone containing high Fe, Cu, Mn, and an edema in the surrounding zone containing lower Cu, Zn and Fe compared to the contralateral hemisphere that was clearly compressed. The water content in the tumour hemisphere was almost homogeneously increased throughout all zones in comparison to the healthy but compressed hemisphere. As first metalloid in the rat brain, arsenic was detected showing a rather homogenous distribution.

6.6. Study of mouse heart tissue by LA-ICP-MS and SIMS

MSI techniques can be applied to study the distribution of metals and biomolecules within tissue sections using MALDI- or DESI-MS [4,32,61]. The synergy of LA-ICP-MS as elemental mass spectrometric imaging technique and SIMS for selected biomolecules was demonstrated firstly in mouse heart tissue [57]. The images of Zn, Fe and Cu measured by LA-ICP-MS and the distribution of choline, phosphocholine and of a cholesterol fragment are shown in Fig. 11. SIMS using a Bi cluster (Bi_n^+) ion source produces secondary ions of atoms and molecules with increased secondary ion yield and low sample penetration depth in the sub-μm range. Therefore, SIMS and LA-ICPMS imaging could be performed subsequently on the same tissue slice [57].

These MSI studies on mouse models could be useful to explain the pathogenesis of coronary heart disease, vascular diseases, systemic arteriosclerosis and plaques formation as a result of changes of metal concentrations.

6.7. Correlation of total Cu distribution and in situ hybridization for coeruloplasmin in the mouse brain

LA-ICP-MS images of metals can be integrated in online multimodal brain atlases such as the Allen-Atlas. This enables a correlation with numerous gene expression profiles. As an example, the Cu image of a sagittal mouse brain section is compared to the coeruloplasmin gene expression profile from Allen Mouse brain atlas in Fig. 12. Note the clusters of high signal in the plexus choroidei of the 3rd and 4th ventricle. This suggests that, as in the liver Cu may be excreted stoichiometrically with coeruloplasmin by the transporter ATP7A that again showed a similar distribution pattern with highest expression in the plexus choroidei.

7. Metallomics studies and mass spectrometric imaging

Metallomics studies using biomolecular MALDI-TOF-MS or MALDI-Fourier transform ion cyclotron mass spectrometry (MALDI-FTICR-MS) and elemental mass spectrometry by LA-ICP-MS were described in series of different papers [1,48,62]. The characterization and identification of several human proteins from brains affected by Alzheimer's disease were analyzed by using the combination of atomic (LA-ICP-MS) and molecular mass spectrometric methods (MALDI-FTICR-MS) after 2D gel electrophoresis. This pioneer research showed the powerful capacity of the combination of high-resolution MALDI-FTICR-MS and LA-ICP-MS for the identification of phosphorylated and metal-containing human

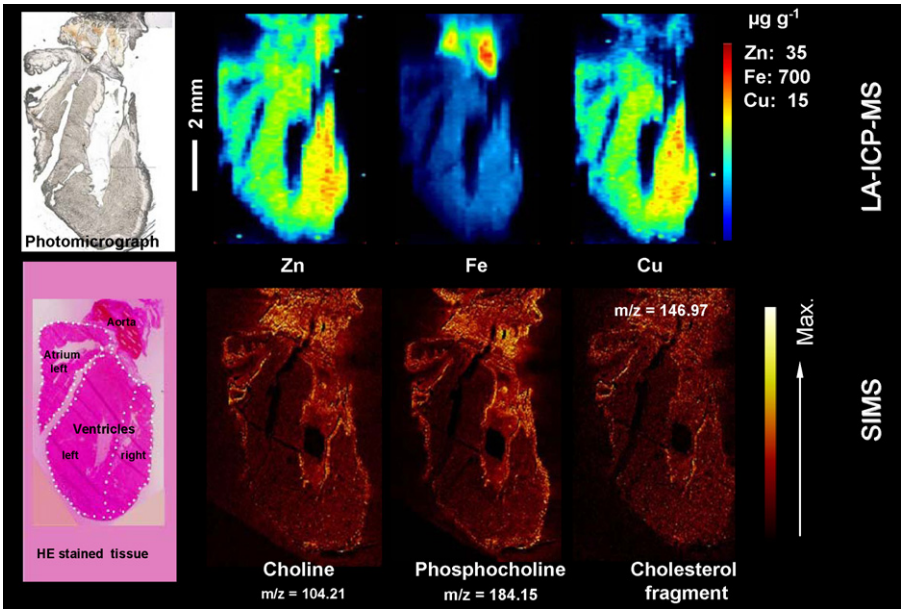

Fig. 11. MSI on mouse heart tissue using LA-ICP-MS and SIMS. Quantitative concentration maps of Zn, Fe and Cu measured by LA-ICP-MS and semi-quantitative ion intensity maps of lipid fragments measured by SIMS are given. Lipids were comparatively low in myocardial tissue and enriched in covering endo- and pericardial tissue. A clearly higher concentration of Fe in the blood was obvious.

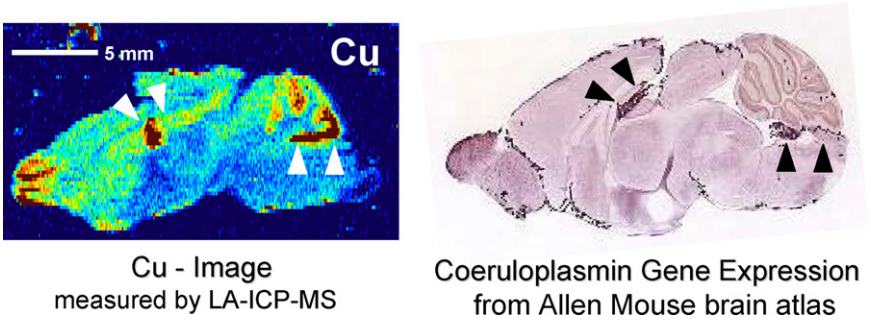

Fig. 12. Cu images of mouse brain compared to coeruloplasmin mRNA (black dots) as retrieved from the Allen Brain Atlas in sagittal sections. Also the Cu transporter ATP7A showed a similar distribution with by far the highest expression in the plexus choroidei of the 3rd and 4th ventricle, labelled by arrowheads.

brain proteins and determination of phosphorus and metal content in selected proteins [62]. Since gel electrophoresis of proteins is a complicated procedure and denaturing processes are involved in SDS–PAGE separation, one should pay attention to both the possible contamination and possible loss of metals in the protein separation. In further studies, non-denaturing protocols such as blue native gel electrophoresis and anodic-PAGE were proposed in several studies and compared with those using denaturing 2D PAGE [32–34]. Recently, Sussilini et al. [63] studied human blood serum samples from bipolar disorder (BD) patients compared to controls after separation of proteins by 2D PAGE. 2D gels were analyzed by LA-ICP-MS bioimaging to detect metals and 32 serum proteins were characterized by MALDI-TOF MS/MS. The identities of the identified proteins were associated with the metals detected previously. Most frequently, Na, Mg, Zn, Ca and Fe were found bounded to proteins in all groups. Mn was limited to the control group, while K and Ti were only found in the BD group. Co was observed only in controls and BD patients treated with Li. P was present in controls and BD patients not treated with Li drugs. This exploratory work suggests the association of LA-ICP-MS with MALDI-TOF-MS/MS as a powerful strategy in metalloproteomic studies applied to determine differences in metal-containing proteins, being able to play an important role on the discovery of potential markers for BD and its treatment with Li.

8. Nano-scale BrainMet techniques

In biological studies there is special interest in the investigation of small regions of tissues and single cells, which requires sensitive and precise analytical techniques with nanometric spatial resolution. BrainMet techniques are now under development for this purpose in author's lab. Two strategies are pursued for the development of nano-scale LA-ICP-MS with high lateral resolution down to low-μm and nm range.

By basing the sample introduction system for a sensitive ICP-MS on a laser micro-dissection (LMD) apparatus with a powerful solid-state laser (see the arrangement in top of Fig. 1), the information of elemental distribution in small sections of biological tissues is achievable at low-μm resolution. For the first time, we combined LMD (SmartCut Plus LMD, MMI Molecular Machines and Industries, Zuerich, Switzerland) directly to a sensitive quadrupole-based mass spectrometer with hexapole collision cell (XSeries2, Thermo Fisher Scientific, Bremen, Germany) for imaging elements in small-sections of brain tissues [42]. In this first application, laser beams from the LMD with different spot sizes (3–5 μm) were used to ablate the sample material which was from a 30-μm-thick brain tissue with a dried Cu droplet in line scan and free-hand scan modes, in order to demonstrated the possibility of the LMD-ICP-MS setup. The inhomogeneous distribution of Cu in the tissue was illustrated

by the changing of ion intensity of Cu along the scanning. A precise determination of the isotope ratio of $^{63}Cu/^{65}Cu$ was also achieved. Due to the much lower laser energy in LMD (1 μJ), the LODs in LMD-ICP-MS were found relatively higher than that of LA-ICP-MS which has a normal energy output of 60–80 μJ for brain tissue analysis. However, the newly developed LMD from MMI with much higher laser energy will be sufficient for the ablation of tissue materials and thereby the analysis by ICP-MS.

On the other hand, we have been establishing a new instrumental arrangement for nano-scale LA-ICP-MS using the optical near-field effect (NF-LA-ICP-MS). The idea consists of inserting a thin Ag needle tip into the radiation field of a defocused laser beam. The tip is controlled by a 3D movement manipulator and the measurement of the tunnel current between the tip and the sample surface. When the tip is brought to the vicinity of the sample surface and works as nano-magnifier around which the radiation field is enhanced causing local laser ablation of the sample surface. The ablated materials are then transported to a sensitive double focusing sector-field mass spectrometer for elemental and isotopic analysis. The physical principles have been illustrated in our previous publications [56–58]. By using NF-LA-ICP-MS setup, various samples including biological tissues and 2D gels, standard reference materials, as well as nanoelectronic devices, were analyzed, showing the possibility and effective measurement by the developed NF-LA-ICP-MS. Fundamental studies of near field enhancement, laser-induced craters on sample surface, as well as the dependency of ion intensity measured by ICP-MS on the tip dimensions and the distance between the tip and the surface, have been intensively investigated [56–58]. It was shown in single-shot measurements that ion intensities of analytes were enhanced significantly by placing the sharp Ag tip very close to the sample surface enabling a precise measurement of isotope ratios. A spatial resolution down to 300 nm can be achieved using NF-LA-ICP-MS. More details of the development and applications of NF-LA-ICP-MS can be found in the review by Wu and Becker in this special issue [24].

9. Future developments and trends in MSI

As shown above, the developed LA-ICP-MS bioimaging techniques have been applied successfully in brain research providing elemental distribution analysis of brain tissue of various types. Other samples such as animal tissues (kidney, liver, spleen, heart, lung, bones and teeth) and plant tissues (leaves, roots, stems and seeds) have also been monitored by LA-ICP-MS bioimaging to study the bioavailability of essential metals, the toxicity of metals and/or the uptake, transport and accumulation of elements in animals and plants [64–67]. However, these element maps only show total element concentrations with no speciation information. Conclusions with respect to biological function so far could be drawn from anatomy. Much more information could be yielded from a tighter link between element and speciation analysis. Increased spatial resolution is the prerequisite for element analysis selective to defined cell types within a tissue or even sub-cellular structures. Therefore major goals of future development are the implementation of techniques allowing several analytical procedures on the same specimen and the increase of spatial resolution. Ongoing BrainMet projects focus on the development of metalloprotein microscopy [52] and nano-scale LA-ICP-MS for imaging of smaller-size biological tissues and single cells [34,68–70].

10. Conclusions

LA-ICP-MS represents an emerging analytical tool for the quantitative imaging of metals combined with metallomic studies in brain research with spatial resolution at the μm scale. The BrainMet techniques developed at Forschungszentrum Jülich can now be used for routine examinations of tissue samples to investigate the function and dysfunction of the nervous system and are also applicable for other biological samples such as sections of plants and animals. LA-ICP-MS techniques with a lateral resolution of nanometers are now under development for the bio-imaging of tissues and cells.

On the other hand, systematic investigations of brain function and neurodegenerative diseases need in particular novel combinations of bioimaging techniques of metals (using LA-ICP-MS) and multimodal molecular imaging (MRI, PET, SPECT, immunostaining, MALDI-MS, SIMS and others). The proposed metalloprotein microscope is an excellent example of combination of advanced elemental and molecular bioimaging techniques, and will bring a bright future for biomedical research.

Acknowledgements

First of all, the first author (JSB) would like to thank Prof. Hans Joachim Dietze (former head of Central Department of Analytical Chemistry, Forschungszentrum Jülich) for his motivating and helpful discussions in this new direction of mass spectrometry. Furthermore JSB would like to thank Prof. Kathryn Morton (Utah University, Salt Lake City) for the ageing studies on mice brain and Prof. Joseph A. Caruso (University of Cincinnati, Cincinnati) for many fruitful and motivating discussions. JSB thank Jürgen Srega and Dr. Meike Hamester (Thermo Fisher Scientific, Bremen) for instrumental support for the BrainMet laboratory and the lab assistant A. Zimmermann (Forschungszentrum Jülich) for technical support with LA-ICP-MS measurements.

References

[1] J.S. Becker, D. Salber, BrainMet—bioimaging of metals in brain and metallomics: new mass spectrometric tools in brain research, Trends Anal. Chem. 29 (2010) 966–978.
[2] W. Shi, M.R. Chance, Metallomics and metalloproteomics, Cell. Mol. Life Sci. (CMLS) 65 (2008) 3040–3048.
[3] A. Sigel, H. Sigel, R.K.O. Sigel, Neurodegenerative Diseases and Metal Ions, John Wiley & Sons, Ltd., Chichester, 2006.
[4] S.S. Rubakhin, J.V. Sweedler, Mass spectrometric imaging: principles and protocols, in: Methods in Molecular Biology, Springer, Heidelberg, 2010.
[5] R. Lobinski, J.S. Becker, H. Haraguchi, B. Sarkar, Metals in biological systems and -omics: guidelines for terminology and critical evaluation of analyical chemistry approaches (IUPAC technical report), Pure Appl. Chem. 82 (2010) 493–504.
[6] L.M. Wang, Q. Wu, J.S. Becker, M.F. Oliveira, F.A. Bozza, A.L. Schwager, M. Lee, J.M. Hoffman, K.A. Morton, Alterations in copper uptake, content and distribution in the brains of aging mice, Metallomics 2 (2010) 348–353.
[7] J.S Becker, M. Zoriy, A. Matusch, B. Wu, D. Salber, C. Palm, J.S. Becker, Bioimaging of metals by LA-ICP-MS, Mass Spectrom. Rev. 29 (2010) 156–175.
[8] J.S. Becker, A. Matusch, C. Palm, D. Salber, K. Morton, J.S. Becker, Bioimaging of metals in brain tissue by laser ablation inductively coupled plasma mass spectrometry (LA-ICP-MS) and metallomics, Metallomics 2 (2010) 104–111.
[9] A. Matusch, C. Depboylu, C. Palm, B. Wu, G.U. Höglinger, M.K.-H. Schäfer, J.S. Becker, Cerebral bio-imaging of Cu, Fe, Zn and Mn in the MPTP mouse model of Parkinson's disease using laser ablation inductively coupled plasma mass spectrometry (LA-ICP-MS), J. Am. Soc. Mass Spectrom. 21 (2010) 161–171.
[10] J.S. Becker, Bioimaging of metals in brain tissue from micrometre to nanometre scale by laser ablation inductively coupled plasma mass spectrometry: state of the art and perspectives, Int. J. Mass Spectrom. 289 (2010) 65–75.
[11] A. Zayed, T. Shoeib, S.E. Taylor, G.D. Jones, A.L. Thomas, J.P. Wood, H.J. Reid, B.L. Sharp, Determination of Pt-DNA adducts and the sub-cellular distribution of Pt in human cancer cell lines and the leukocytes of cancer patients, following mono- or combination treatments, by inductively-coupled plasma mass spectrometry, Int. J. Mass Spectrom., this issue.
[12] G. Zhang, W. Hu, Z. Du, S. Lv, Q. Iuo, X. Li, K. Wu, Y. Han, F. Wang, A comparative study on interactions of cisplatin and ruthenium arene anticancer complexes with metallothionein using MALDI-TOF-MS, Int. J. Mass Spectrom., this issue.
[13] K. Nakazato, T. Nagamine, K. Suzuki, T. Kusakabe, H.D. Moon, M. Oikawa, T. Sakai, K. Arakawa, Suncellular changes of essential metal shown by microPIXE in oral cadmium-exposed mice, BioMetals 21 (2008) 83–91.
[14] H.R. Pohl, H.G. Abadin, J.F. Risher, Neurotoxicity of cadmium, lead and mercury, in: H.S.A. Sigel, R.K.O. Sigel (Eds.), Metal Ions in Life Sciences, Wiley and Sons, Chichester, 2006, pp. 395–425.

[15] D.J. Bellis, D. Li, Z. Chen, W.M. Gibson, P.J. Parsons, Measurement of the microdistribution of strontium and lead in bone via benchtop monochromatic microbeam X-ray fluorescence with a low power source, J. Anal. At. Spectrom. 24 (2009) 622–626.
[16] W. Ribi, T.J. Senden, A. Sakellariou, A. Limayec, S. Zhang, Imaging honey bee brain anatomy with micro-X-ray-computed tomography, J. Neurosci. Methods 171 (2008) 93–97.
[17] L.M. Miller, Q. Wang, T.P. Telivala, R.J. Smith, A. Lanzirotti, J. Miklossy, Synchrotron-based infrared and X-ray imaging shows focalized accumulation of Cu and Zn co-localized with beta-amyloid deposits in Alzheimer's disease, J. Struct. Biol. 155 (2006) 30–37.
[18] T. Punshon, B.P. Jackson, A. Lanzirotti, W.A. Hopkins, P.M. Bertsch, J. Burger, Application of synchrotron X-ray microbeam spectroscopy to the determination of metal distribution and speciation in biological tissues, Spectrosc. Lett. 38 (2005) 343–363.
[19] B. De Samber, R. Evens, K. De Schamphelaere, G. Silversmit, B. Masschaele, T. Schoonjans, B. Vekemans, C. Janssen, L. Van Hoorebeke, I. Szaloki, L. Balcaen, F. Vanhaecke, G. Falkenberg, L. Vincze, Combining synchrotron and laboratory X-ray techniques for studying tissue-specific trace level metal distributions in daphnia magna, J. Anal. At. Spectrom. 23 (2008) 829–839.
[20] A. Carmona, P. Cloetens, G. Devès, S. Bohic, R. Ortega, Nano-imaging of trace metals by synchrotron X-ray fluorescence into dopaminergic single cells and neurite-like processes, J. Anal. At. Spectrom. 23 (2008) 1083–1088.
[21] S. Chandra, 3D subcellular SIMS imaging in cryogenically prepared single cells, Appl. Surf. Sci. 231 (2004) 467–469.
[22] J.L. Guerquin-Kern, T.D. Wu, C. Quintana, A. Croisy, Progress in analytical imaging of the cell by dynamic secondary ion mass spectrometry (SIMS microscopy), Biochim. Biophys. Acta—Gen. Subjects 1724 (2005) 228–238.
[23] M.A. Heeren, L.A. Mc Donnell, E. Amstalden, S.L. Luxambourgh, A.F.M. Altelaar, S.R. Piersma, Why don't biologists use SIMS? A critical evaluation of imaging MS, Appl. Surf. Sci. 252 (2006) 6827–6835.
[24] S. Chandra, W. Tjarks, D.R. Lorey, R.F. Barth, Quantitative subcellular imaging of boron compounds in individual mitotic and interphase human glioblastoma cells with imaging secondary ion mass spectrometry (SIMS), J. Microsc. 229 (2007) 92–103.
[25] T.G. Lee, J.W. Parka, H.K. Shona, D.W. Moon, W.W. Choib, K. Lib, J.H. Chung, Biochemical imaging of tissues by SIMS for biomedical applications, Appl. Surf. Sci. 255 (2008) 1241–1248.
[26] J.A. McLean, W.B. Ridenour, R.M. Caprioli, Profiling and imaging of tissues by imaging ion mobility-mass spectrometry, J. Mass Spectrom. 42 (2007) 1099–1105.
[27] M. Stoeckli, P. Chaurand, D.E. Hallahan, R.M. Caprioli, Imaging mass spectrometry: a new technology for the analysis of protein expression in mammalian tissues, Nat. Med. 7 (2001) 493–496.
[28] P.J. Todd, T.G. Schaaf, P. Chaurand, R.M. Caprioli, Organic ion imaging of biological tissue with secondary ion mass spectrometry and matrix-assisted laser desorption/ionization, J. Mass Spectrom. 36 (2001) 355–369.
[29] W.B. Ridenour, M. Kliman, J.A. McLean, R.M. Caprioli, Structural characterization of phospholipids and peptides directly from tissue sections by MALDI traveling-wave ion mobility-mass spectrometry, Anal. Chem. 82 (2010) 1881–1889.
[30] S.R. Oppenheimer, D.M. Mi, M.E. Sanders, R.M. Caprioli, Molecular analysis of tumor margins by MALDI mass spectrometry in renal carcinoma, J. Proteome Res. 9 (2010) 2182–2190.
[31] J.L. Norris, D.S. Cornett, J.A. Mobley, M. Andersson, E.H. Seeley, P. Chaurand, R.M. Caprioli, Processing MALDI mass spectra to improve mass spectral direct tissue analysis, Int. J. Mass Spectrom. 260 (2007) 212–221.
[32] M. Girod, Y. Shi, J.X. Chen, R.G. Cooks, Desorption electrospray ionization imaging mass spectrometry of lipids in rat spinal cord, J. Am. Soc. Mass Spectrom. 21 (2010) 1177–1189.
[33] J.M. Wiseman, D.R. Ifa, Q. Song, R.G. Cooks, Tissue imaging at atmospheric pressure using desorption electrospray ionization (DESI) mass spectrometry, Angew. Chem. 43 (2006) 7346–7350.
[34] B. Wu, J.S. Becker, Chemical imaging of biological tissues and cells in the low-micrometer and nanometer range, Int. J. Mass Spectrom., this special issue.
[35] R.W. Hutchinson, A.G. Cox, C.W. McLeod, P.S. Marshall, A. Harper, E.L. Dawson, D.R. Howlett, Imaging and spatial distribution of beta-amyloid peptide and metal ions in Alzheimer's plaques by laser ablation-inductively coupled plasma-mass spectrometry, Anal. Biochem. 346 (2005) 225–233.
[36] B. Jackson, S. Harper, L. Smith, J. Flinn, Elemental mapping and quantitative analysis of Cu, Zn, and Fe in rat brain sections by laser ablation ICP-MS, Anal. Bioanal. Chem. 384 (2006) 1618–2642.
[37] L.A. McDonnell, S.R. Piersma, A.F.M. Altelaar, T.H. Mize, S.L. Luxembourg, P.D.E.M. Verhaert, J. van Minnen, R.M.A. Heeren, Subcellular imaging mass spectrometry of brain tissue, J. Mass Spectrom. 40 (2005) 160–168.
[38] J. Dobrowolska, M. Dehnhardt, A. Matusch, M. Zoriy, P. Koscielniak, K. Zilles, J.S. Becker, Quantitative imaging of zinc, copper and lead in three distinct regions of the human brain by laser ablation inductively coupled plasma mass spectrometry, Talanta 74 (2008) 717–723.
[39] J.S Becker, M. Zoriy, B. Wu, A. Matusch, B.J. Su, Imaging of essential and toxic elements in biological tissues by LA-ICP-MS, J. Anal. At. Spectrom. 23 (2008) 1275–1280.
[40] J.S. Becker, A. Matusch, C. Depboylu, J. Dobrowolska, M. Zoriy, Quantitative imaging of selenium, copper, and zinc in thin sections of biological tissues (Slugs-Genus arion) measured by laser ablation inductively coupled of plasma mass spectrometry, Anal. Chem. 79 (2007) 6074–6080.
[41] J.S. Becker, M. Zoriy, C. Pickhardt, N. Palomero-Gallagher, K. Zilles, Imaging of copper, zinc, and other elements in thin section of human brain samples (Hippocampus) by laser ablation inductively coupled plasma mass spectrometry, Anal. Chem. 77 (2005) 3208–3216.
[42] M. Dehnhardt, M. Zoriy, Z. Khan, G. Reifenberger, T.J. Ekstrom, J.S. Becker, K. Zilles, A. Bauer, Element distribution is altered in a zone surrounding human glioblastoma multiforme, J. Trace Elem. Med. Biol. 22 (2008) 17–23.
[43] M. Zoriy, M. Dehnhardt, A. Matusch, J.S. Becker, Comparative imaging of P, S, Fe, Cu, Zn and C in thin sections of rat brain tumor as well as control tissues by laser ablation inductively coupled plasma mass spectrometry, Spectrochim. Acta B 63 (2008) 375–382.
[44] J.S. Becker, M. Zoriy, M. Dehnhardt, C. Pickhardt, K. Zilles, Copper, zinc, phosphorus and sulfur distribution in thin section of rat brain tissues measured by laser ablation inductively coupled plasma mass spectrometry: possibility for small-size tumor analysis, J. Anal. At. Spectrom. 20 (2005) 912–917.
[45] M. Zoriy, M. Dehnhardt, G. Reifenberger, K. Zilles, J.S. Becker, Imaging of Cu, Zn, Pb and U in human brain tumor resections by laser ablation inductively coupled plasma mass spectrometry, Int. J. Mass Spectrom. 257 (2006) 27–33.
[46] L.M. Wang, J.S. Becker, Q. Wu, M.F. Oliveira, F.A. Bozza, A.L. Schwager, J.M. Hoffman, K.A. Morton, Alterations in copper uptake, content and distribution in the brains of aging mice, Metallomics 2 (2010) 348–353.
[47] D. Pozebon, V. Dressler, A. Matusch, J.S. Becker, Monitoring of platinum in a single hair by laser ablation inductively coupled plasma mass spectrometry (LA-ICP-MS) after cisplatin, Int. J. Mass Spectrom. 272 (2008) 57–62.
[48] J.S. Becker, R. Lobinski, J.S. Becker, Metal imaging in non-denaturating 2D electrophoresis gels by laser ablation inductively coupled plasma mass spectrometry (LA-ICP-MS) for the detection of metalloproteins, Metallomics 1 (2009) 312–316.
[49] J.S. Becker, D. Pozebon, V.L. Dressler, R. Lobinski, J.S. Becker, LA-ICP-MS studies of zinc exchange by copper in bovine serum albumin using an isotopic enriched copper tracer, J. Anal. At. Spectrom. 23 (2008) 1076–1082.
[50] M. Zoriy, M. Kayser, A. Izmer, C.B.J.S. Pickhardt, Determination of uranium isotopic ratios in biological samples using laser ablation inductively coupled plasma double focusing sector field mass spectrometry with cooled ablation chamber, Int. J. Mass Spectrom. 242 (2005) 297–302.
[51] J.S. Becker, U. Kumtabtim, B. Wu, P. Steinacker, M. Otto, A. Matusch, Bioimaging of metals in mouse spinal cord by laser ablation inductively coupled plasma mass spectrometry, (2011), submitted for publication.
[52] J.S. Becker, S. Niehren, A. Matusch, B. Wu, H.-F. Fang, U. Kumtabtim, M. Hamester, D. Salber, Scaling down the bioimaging of metals by laser microdissection inductively coupled plasma mass spectrometry (LMD-ICP-MS), Int. J. Mass Spectrom. 294 (2010) 1–6.
[53] T. Osterholt, D. Salber, A. Matusch, J.S. Becker, C. Palm, IMAGENA: image generation and analysis—an interactive software tool handling LA-ICP-MS data, Int. J. Mass Spectrom., this issue (2011).
[54] V.L. Dressler, D. Pozebon, M. Foster Mesko, A. Matusch, U. Kumtabtim, B. Wu, J.S. Becker, Biomonitoring of essential and toxic metals in single hair using on-line solution-based calibration in laser ablation inductively coupled plasma mass spectrometry, Talanta 82 (2010) 1770–1777.
[55] D. Pozebon, V.L. Dressler, M.F. Mesko, A. Matusch, J.S. Becker, Bioimaging of metals in thin mouse brain section by laser ablation inductively coupled plasma mass spectrometry: novel online quantification strategy using aqueous standards, J. Anal. At. Spectrom. 25 (2010) 1739–1744.
[56] G. Paxinos, C. Watson, The Rat Brain in Stereotaxic Coordinates, Academic Press/Elsevier, Amsterdam/Boston, 2007.
[57] J.S. Becker, U. Breuer, H.-F. Hsieh, T. Osterholt, U. Kumtabtim, B. Wu, A. Matusch, J.A. Caruso, Z. Qin, Bioimaging of metals and biomolecules in mouse heart by laser ablation inductively coupled plasma mass spectrometry and secondary ion mass spectrometry, Anal. Chem. 82 (2010) 9528–9533.
[58] T. Kral, H. Clusmann, J. Urbach, J. Schramm, C.E. Elger, M. Kurthen, T. Grunwald, Preoperative evaluation for epilepsy surgery, Zentralbl. Neurochir. 63 (2002) 106–110.
[59] M. Majores, S. Schoch, A.B.A.J. Lie, Molecular neuropathology of temporal lobe epilepsy: complementary approaches in animal models and human disease tissue, Epilepsia 48 (2007) 4–12.
[60] A. Matusch, A. Bauer, J.S. Becker, Element imaging in formalin fixed slices of human mesencephalon, Int. J. Mass Spectrom., this issue (2011).
[61] B.D. Corbin, E.H. Seeley, A. Raab, J. Feldmann, M.R. Miller, V.J. Torres, K.L. Anderson, B.M. Dattilo, P.M. Dunman, R. Gerads, R.M. Caprioli, W. Nacken, W.J. Chazin, E.P. Skaar, Metal chelation and inhibition of bacterial growth in tissue abscesses, Science 319 (2008) 962–965.
[62] J.S. Becker, M. Zoriy, M. Przybylski, J.S. Becker, Study of formation of Cu- and Zn-containing tau protein using isotopic-enriched tracers by LA-ICP-MS and MALDI-FTICR-MS, J. Anal. At. Spectrom. 22 (2007) 63–68.
[63] A. Sussulini, H. Kratzin, O. Jahn, C.E. Muller Banzato, M.A.Z. Arruda, J.S. Becker, Metallomics studies of human blood serum from treated bipolar disorder patients, Anal. Chem. 82 (2010) 5859–5864.
[64] B. Wu, M. Zoriy, Y. Chen, J.S. Becker, Imaging of nutrient elements in the leaves of Elsholtzia splendens by laser ablation inductively coupled plasma mass spectrometry (LA-ICP-MS), Talanta 78 (2009) 132–137.
[65] M.C. Santos, M. Wagner, B. Wu, J. Scheider, J. Oehlmann, S. Cadore, J.S. Becker, Biomonitoring of metal contamination in a marine prosobranch snail (Nassarius reticulatus) by imaging laser ablation inductively coupled plasma mass spectrometry (LA-ICP-MS), Talanta 80 (2009) 423–430.

[66] B. Wu, Y. Chen, J.S. Becker, Study of essential element accumulation in the leaves of a Cu-tolerant plant Elsholtzia splendens after Cu stress by imaging LA-ICP-MS, Anal. Chim. Acta 633 (2009) 165–172.
[67] J.S. Becker, R.C. Dietrich, A. Matusch, D. Pozebon, V.L. Dressler, Quantitative images of metals in plant tissues measured by laser ablation inductively coupled plasma mass spectrometry, Spectrochim. Acta B (2008).
[68] J.S. Becker, A. Gorbunoff, M. Zoriy, A. Izmer, M. Kayser, Evidence of near-field laser ablation inductively coupled plasma mass spectrometry (NF-LA-ICP-MS) at nanometre scale for elemental and isotopic analysis on gels and biological samples, J. Anal. At. Spectrom. 21 (2006) 19–25.
[69] M. Zoriy, J.S. Becker, Near-field laser ablation inductively coupled plasma mass spectrometry (LA-ICP-MS): A novel elemental analytical technique at nanometer scale, Rapid Commun. Mass Spectrom. 23 (2009) 23–30.
[70] M. Zoriy, M. Kayser, J.S. Becker, Possibility of nano-local element analysis by near-field laser ablation inductively coupled plasma mass spectrometry (LA-ICP-MS): new experimental arrangement and first application, Int. J. Mass Spectrom. 273 (2008) 151–155.